THE JOURNAL OF PHYSICAL CHEMISTRY C

Article

pubs.acs.org/JPCC

Energetics of Confinement of *n*-Hexane in Ca–Na Ion Exchanged Zeolite A

Hui Sun,[†,‡,§] Di Wu,[‡,§] Xiaofeng Guo,[‡] Benxian Shen,[†] Jichang Liu,[†] and Alexandra Navrotsky*[,‡]

[†]State Key Laboratory of Chemical Engineering, East China University of Science and Technology, Shanghai 200237, P. R. China

[‡]Peter A. Rock Thermochemistry Laboratory and NEAT ORU, University of California Davis, Davis, California 95616, United States

ABSTRACT: Study of the energetics of confinement of small organic molecules in microporous frameworks provides essential information for rational design and application of functional porous materials. Using immersion calorimetry and temperature-programmed desorption coupled with mass spectroscopy, we describe the complex guest–host interactions of a nonpolar organic molecule (*n*-hexane) with a series of calcium-exchanged zeolite A materials whose pore accessibility was modified by varying the calcium content to achieve inaccessible, partially accessible, and fully accessible central cavities for *n*-hexane molecules. The overall magnitude and trend with the pore size of *n*-hexane–zeolite A interactions have been determined. In addition, the contributions to energetics from the external surface (ΔH_{wet}), tetrahedral framework ($\Delta H_{g\text{-}h}$), and adjacent *n*-hexane molecules ($\Delta H_{g\text{-}g}$) were separated, quantified, and interpreted.

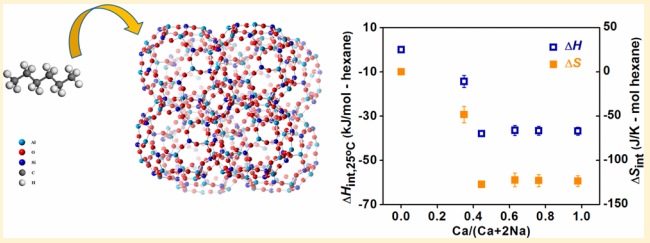

1. INTRODUCTION

Because of their periodic and ion-balanced structures with defined and controllable pore sizes and abundant internal surface area, zeolites have been widely used in scientific research and technological applications, including adsorption, shape selective catalysis, ion exchange, and medical treatment.[1−4] In such applications, the interactions between guest species and host frameworks are crucial governing factors in determining properties.[5] A large number of studies, both theoretical and experimental, have been carried out to explore such interactions.[6−8] The energetics of *n*-alkane confinement in zeolites has been studied by molecular modeling.[9,10] Static and dynamic experimental methods have been employed as well, in which the physical chemistry of molecule–zeolite interactions has been discussed.[11−14] However, most of these studies used specific host frameworks and guest molecules, without a systematic variation of parameters to define the fundamental interactions.

Solution and immersion calorimetry are powerful techniques to obtain interaction enthalpies in guest–host systems. Initial studies focused on confinement of embedded structural directing agents (SDAs) in as-made zeolites and on water–cation–zeolite interactions. Eder et al. investigated alkane sorption in molecular sieves and discussed the contributions from ordering, intermolecular interactions, and Brönsted acid sites.[7] Recently, interactions of small guest molecules (water, ethanol, and triethylamine) with a series of mesoporous silicas were quantified at room temperature using immersion calorimetry.[15] Wu et al. employed hydrofluoric acid (HF) solution calorimetry to investigate energetics and phase evolution of a rigid, spherical organic molecule confined in mesoporous silicas with different pore sizes.[16] The adsorption energetics were also studied for several metal–organic frameworks (MOFs) using microcalorimetry.[19,20]

With its α cage aperture modifiable by fine-tuning the degree of calcium exchange, zeolite A offers a well-defined structure for molecular confinement study (see Figure 1). Despite the wide use of zeolite A in the separation of linear and branched alkanes,[21,22] the interactions between alkanes and calcium-exchanged zeolite A have not been characterized in detail. The contributions from various types of interactions among the guest molecule, the framework, and the cation (Na or Ca), though recognized as important,[23−25] have not been separated and quantified. In the present study, the magnitudes of guest–host interactions between *n*-hexane and calcium-exchanged zeolite A were determined using immersion calorimetry coupled with temperature-programmed desorption and mass spectroscopy (TPD–MS). The objective is to quantify the energetics of *n*-hexane adsorption/confinement in Ca-exchanged zeolite A, to separate contributions from various factors (surface, framework, cation, and intermolecular interactions), and finally to understand and generalize the systematics of confinement of nonpolar hydrocarbon molecules in zeolites.

2. EXPERIMENTAL METHODS

2.1. Preparation of Ca-Exchanged Zeolite A. Synthetic zeolite Na-A (RM 8851), obtained from the National Institute of Standards and Technology (NIST) was used as starting material. Ion exchange was performed by immersing 2.0 g of

Received: August 22, 2014
Revised: October 14, 2014
Published: October 14, 2014

   dx.doi.org/10.1021/jp508514e | J. Phys. Chem. C 2014, 118, 25590–25596

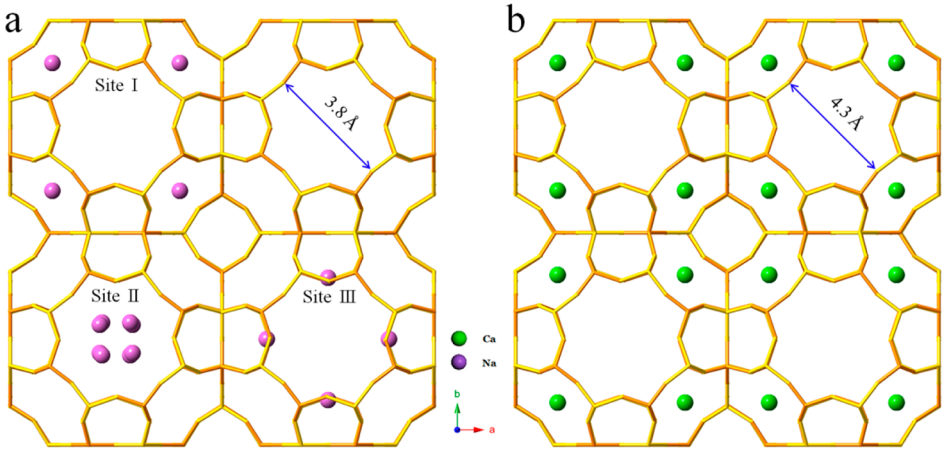

Figure 1. Framework structures of zeolites (a) Na-A and (b) Ca-A. Site I, Site II, and Site III in (a) indicate the cation sites occupied by adjacent sodium ions. Na-A: space group $Fm\bar{3}c$, cell parameter a = 24.555 Å.[17] Ca-A: space group $Fm\bar{3}c$, cell parameter a = 24.47 Å.[18]

zeolite Na-A in 40 mL of $CaCl_2$ aqueous solution (0.05−0.25 M) kept at 80 °C under vigorous stirring for 24 h. The solid products were washed at least three times with deionized water and separated by centrifugation. To achieve a fully Ca-exchanged zeolite A, this procedure was triplicated. The ion-exchanged samples were dried at 120 °C overnight and stored in a tightly sealed desiccator with 33 ± 2% relative humidity, generated by a saturated $MgCl_2$ aqueous solution at room temperature, for at least 2 days before any characterization. Prior to immersion calorimetry, the samples were heated from room temperature to 450 °C at 10 °C/min and kept at 450 °C under vacuum (10^{-4} Torr) for 16 h using the degas port of a gas adsorption analyzer (Micromeritics ASAP 2020).

Samples saturated with *n*-hexane were prepared by a vapor deposition method, in which the dehydrated frameworks were placed in a tightly sealed desiccator together with a small vial of liquid *n*-hexane (99.9% purity, Fisher Scientific). Although liquid *n*-hexane did not directly contact the samples, its saturation vapor at room temperature diffused into the void spaces in the frameworks and was confined. The saturation process was performed for at least 2 days. Then, these equilibrated *n*-hexane-containing samples were used for temperature-programmed desorption mass spectrometry (TPD−MS) analyses.

2.2. Characterization. Powder X-ray diffraction (XRD) patterns were collected at room temperature using a Bruker-AXS D8 Advance X-ray diffractometer operated at 40 kV and 40 mA with Cu Kα radiation. Data were recorded from 5−60° with a step size of 0.02° and 1 s·step^{-1}. Lattice parameter a was refined using Jade 6.0 and the ICSD database.

The chemical compositions were determined using a Cameca SX-100 electron microprobe with a beam current of 10 nA and an accelerating voltage of 15 kV. Sample pellets were embedded in a plastic holder with epoxy resin and polished with diamond paste. Eight points were measured on each specimen. Homogeneity was checked using backscattered electron (BSE) imaging.

2.3. Temperature-Programmed Desorption Mass Spectrometry (TPD−MS). TPD−MS analyses were performed on a Netzsch STA 449 system coupled with mass spectrometry to determine the contents of *n*-hexane in each sample. Sample pellets weighing about 20 mg were placed in a platinum crucible and heated under an argon flow (40 mL/min) from 30 to 600 °C at 10 °C/min. The TPD exhaust species were collected into the ionization chamber of a Micromeritics Cirrus 2 quadrupole mass spectrometer, ionized, and fragmented by electron impact. Their m/z values were identified, and the ion currents from desorption and pyrolysis products were recorded with an electron multiplier. The contents of adsorbed/confined *n*-hexane were derived from integration of the corresponding carbon species peaks in the mass spectra. Blank runs were performed without a zeolite sample as the baseline. All sample MS traces were corrected with that baseline before peak integration. The mass spectrometer was calibrated using zeolite samples with known water contents. TPD−MS analyses were triplicated on zeolite Na-A, which had been equilibrated under 33 ± 2% relative humidity created by a saturated $MgCl_2$ aqueous solution to obtain an average calibration factor for the amount of water in the samples.

2.4. Immersion Calorimetry. The enthalpies of immersion of zeolite CaNa-A in liquid *n*-hexane were determined using a Setaram C-80 twin microcalorimeter equipped with a custom-made glass dropping tube. Dehydrated samples were pressed into pellets (∼10 mg) and dropped into *n*-hexane maintained at 25 ± 0.5 °C. The drop generated a heat effect associated with the contact and confinement of *n*-hexane with the zeolite sample. A typical measurement took 45−90 min. The measurement on each sample was repeated 4−8 times to ensure reproducibility.

3. RESULTS

3.1. Structure and Composition of Zeolite Na-A and CaNa-A. The powder XRD patterns for calcium-exchanged zeolite A are shown in Figure 2. All samples are confirmed to be single phase. The present observations agree with a previous report,[26] which suggests that the lattice parameter a is closely correlated to the calcium content (Table 1).

The chemical compositions and calculated molar mass (per mole of TO_2) of Ca-exchanged zeolite A are listed in Table 1. The Si/Al ratio of all samples is identical (1.03 ± 0.01), which is very close to that of ideal zeolite A. This is strong indication of consistent high framework quality after ion exchange, with no degradation of the materials. The Ca exchange ranges from 34.8 to 97.9 mol % (see Table 1).

3.2. TPD−MS. The TPD−MS profiles for dehydration of zeolite Na-A are shown in Figure 3. Applying Gaussian multipeak fitting, both the differential thermogravimetric

dx.doi.org/10.1021/jp508514e | J. Phys. Chem. C 2014, 118, 25590−25596

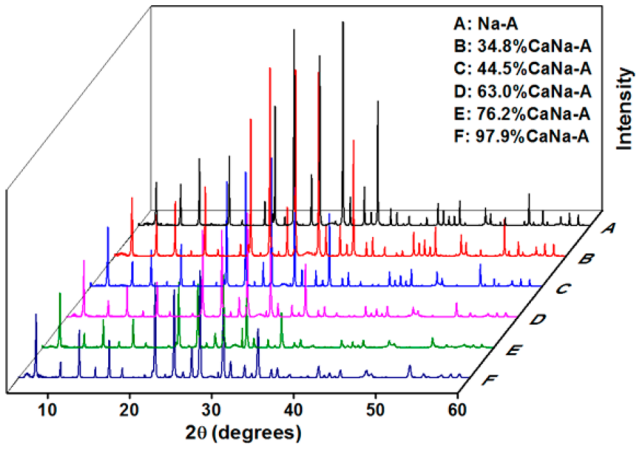

Figure 2. Powder X-ray diffraction (XRD) patterns of zeolites Na-A and CaNa-A. Values in front of CaNa-A denote the degree of exchange.

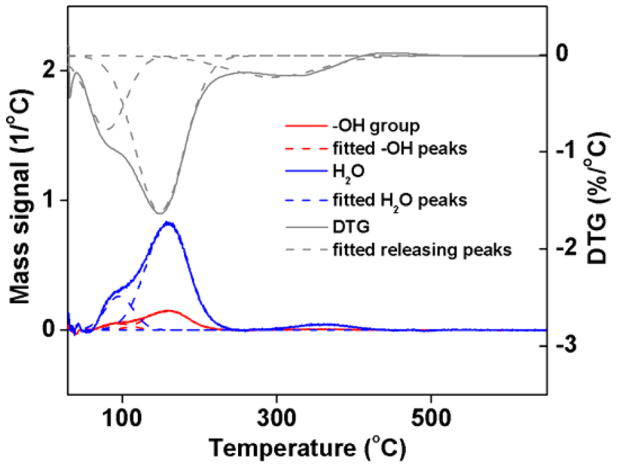

Figure 3. Differential thermogravimetric analysis (DTG) and mass spectroscopy (MS) profiles for hydrated zeolite Na-A.

(DTG) and MS traces are separated into three peaks (Figure 3). The well-resolved MS peaks of H_2O and −OH have nearly identical shapes and positions as those on the DTG curves. Therefore, the overall water content can be integrated from both of the peaks on the MS and TGA curves (see Table 2). In addition, the average calibration factor was calculated by dividing the overall area of water species on the MS trace $A_{H_2O} + A_{-OH}$, over the amount of desorbed water, w_{H_2O}. All three sets of the TPD−MS experiment show highly consistent results.

Applying the calibration factor to the TGA weight loss, we were able to calculate the contents of water and hexane for each sample. With consideration of MS signals from all the carbon-containing species (Figure 4), the amounts of *n*-hexane confined in 34.8% and 63.0% CaNa-A are 0.44 and 1.45 mmol/g (0.038 and 0.125 g per g of zeolite) (see Table 3). Both of these values are in good agreement with our previous measurements (see Table 4) using a static binary mixture solution method (0.43 mmol/g for 34.3% CaNa-A and 1.45 mmol/g for 64.0% CaNa-A at 25 °C,[27] 1.48 mmol/g for CaNa-A at 20 °C[28]), and with other works (1.44 mmol/g at 26 °C[29] and a maximum of 1.51 mmol/g[30,31]).

The MS profiles of 34.8% and 63.0% CaNa-A are presented in Figure 5. The signals of propyl (m/z = 43), butyl (m/z = 57), and pentyl groups (m/z = 71) and hexane (m/z = 86) are all assigned as coming from *n*-hexane. Each signal shows two well-resolved peaks at about 100 and 200−300 °C. Applying Gaussian multipeak fitting, ratios of these two peaks are 0.85 for 34.8% CaNa-A, and 0.30 for 63.0% CaNa-A. Interestingly, for zeolite A with a higher calcium content, this value remains the same, 0.30.

Table 2. TPD−MS Calibration on Hydrated Zeolite Na-A Samples

$m_{hyd\text{-}zeolite}$[a], mg	x[b], wt %	w_{H_2O}[c], mg	A_{H_2O}[d]	A_{-OH}[e]	F[f], mg^{-1}
8.67	19.55	1.69	122.49	21.94	85.21
10.51	18.71	1.97	144.47	25.85	86.62
11.36	19.95	2.27	162.37	29.37	84.61

[a]Weight of hydrated zeolite Na-A equilibrated under 33 ± 2% relative humidity. [b]TGA weight loss relative to hydrated zeolite samples in the integral temperature region. [c]Amount of water released in the integral temperature region. [d]Relative integral area for three peaks related to H_2O on the MS profiles. [e]Relative integral areas for three −OH group peaks on the MS profiles. [f]Average calibration factor for TPD−MS quantitative analysis.

3.3. Immersion Calorimetry. The enthalpies of immersion for zeolite A in *n*-hexane liquid are listed in Table 4. Values for Ca-exchanged zeolite A are more exothermic than those for zeolite A in its sodium form. The heat of immersion for samples with more than 63.0% calcium exchange (~59 J/g - zeolite) agrees with a previously reported value for zeolite Ca-A (61 J/g - zeolite).[32] Na-A has the least exothermic enthalpy of immersion of −0.39 ± 0.025 kJ/mol - TO_2 (−5.59 ± 0.35 J/g - zeolite), whereas zeolites with more than 44.5% calcium appear more exothermic with values from −4.06 ± 0.09 (−57.18 ± 1.29 J/g - zeolite) to −4.12 ± 0.21 kJ/mol - TO_2 (−58.70 ± 2.96 J/g - zeolite).

The effective aperture diameter of zeolite Na-A (3.8 Å) is too narrow for the *n*-hexane molecule (kinetic diameter: 4.3 Å) to enter the central (α) cavity (see Figure 1).[5] Therefore, the measured immersion enthalpy for Na-A represents only wetting of its external surface by *n*-hexane (wetting heat). Because of

Table 1. Chemical Compositions of Zeolites Na-A and CaNa-A (per Mole of TO_2)

zeolite	chemical composition	MW (g)	a [Å][b]
Na-A	$Na_{0.480}Al_{0.491}Si_{0.509}O_{1.995}$	70.48	24.6187(3)
34.8%CaNa-A[a]	$Na_{0.296}Ca_{0.079}Al_{0.490}Si_{0.510}O_{1.982}$	69.24	24.6412(3)
44.5%CaNa-A[a]	$Na_{0.287}Ca_{0.115}Al_{0.494}Si_{0.506}O_{2.011}$	70.92	24.6464(7)
63.0%CaNa-A[a]	$Na_{0.182}Ca_{0.154}Al_{0.497}Si_{0.503}O_{1.997}$	69.85	24.6385(3)
76.2%CaNa-A[a]	$Na_{0.121}Ca_{0.194}Al_{0.490}Si_{0.510}O_{2.010}$	70.27	24.6262(2)
97.9%CaNa-A[a]	$Na_{0.011}Ca_{0.249}Al_{0.490}Si_{0.510}O_{2.010}$	69.94	24.5606(9)

[a]The values in front of CaNa-A denote the degrees of calcium exchange of CaNa-A samples. [b]Lattice parameter.

dx.doi.org/10.1021/jp508514e | J. Phys. Chem. C 2014, 118, 25590−25596

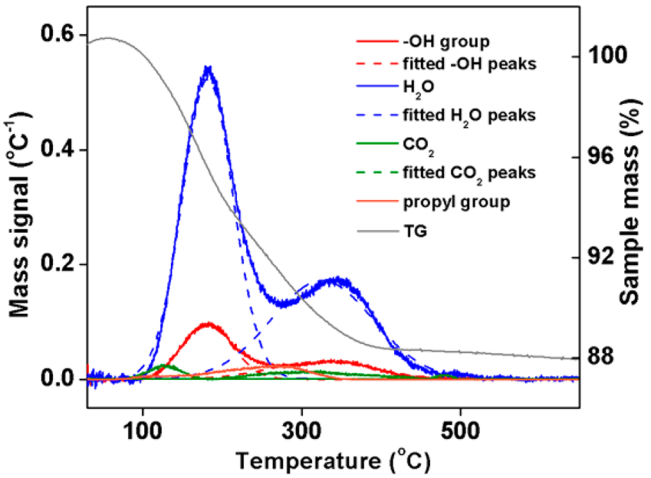

Figure 4. Temperature-programmed desorption mass spectrometry (TPD−MS) profiles for 34.8% CaNa-A sample.

the negligible changes in external surface area during ion exchange, the wetting amounts and wetting heats of all samples can be considered to be identical. The amount of *n*-hexane involved in the wetting process was found to be 1.93 mmol/g (see Table 4). The heat of wetting was measured as −2.90 ± 0.18 kJ/mol - hexane, which is comparable to the wetting heats (*n*-hexane) of other inorganic porous materials.[33] The Q_c values in Table 4 show that the average number of *n*-hexane molecules confined in one α cage increases with calcium content from zero for Na-A, to 0.7 for 34.8% CaNa-A. All samples with higher calcium contents (44.5, 63.0, 76.2, and 97.9% CaNa-A) have nearly equal numbers of confined *n*-hexane molecules (2.4 per α cage).

After subtracting the wetting heat and using results from TPD−MS and immersion calorimetry, we are able to calculate the enthalpy of interaction, which is defined as the energetic effect associated with confinement of *n*-hexane in the pores of Ca-exchanged zeolite A (see Figure 6). The enthalpy of interaction becomes more exothermic until reaching a plateau of about −36.5 kJ/mol - hexane. These enthalpies of interaction correspond well to the heat of adsorption of *n*-hexane at low coverage (around −35 kJ/mol - hexane with respect to vaporization enthalpy of *n*-hexane at 100 °C), extracted from gas adsorption isotherms.[30,34]

4. DISCUSSION

In each zeolite A pseudo-cell, there are 12 net negative charges, which have to be balanced by cations.[35] These high-energy sites have distinct crystallographic positions and are classified into three categories: site I, centered in the six-membered rings (6MR) and displacing into the α cavity; site II, located near the center of the eight-membered rings (8MR) and being close to its planes; and site III, centered in the four-membered rings (4MR) and displacing into the α cavity. Accordingly, the charge balancing sodium cations in zeolite Na-A are located at these 12 sites and can be substituted by other cations such as calcium. Specifically, in Na-A, 8 of the 12 Na^+ are at sites I (6MR), 3 at sites II (8MR), and the remaining 1 at sites III (4MR).[17,36] In this scenario, all the 6 8MR windows are partially blocked by Na^+, resulting in a reduced effective aperture diameter, from 4.3 Å (cation-vacant) to 3.8 Å (sodium-occupied) (see Figure 1). This small difference in size creates severe steric hindrance, blocking access of *n*-hexane molecules into the central cages of Na-A. In other words, interaction of Na-A with *n*-hexane mainly happens on the external surface of the zeolite and is simply wetting.

Once 2 Na^+ are exchanged by 1 Ca^{2+}, the total number of cations in zeolite A decreases. In fact, each cation has its site selectivity; Ca^{2+} cations prefer sites I. Site II, which locates near the center of 8MR, is filled by Ca^{2+} only if there are more than 8 cations (Na^+ and Ca^{2+} in total) per cell (once sites I are entirely filled).[37,38] For the 34.8% CaNa-A, about 6 Na^+ and 2 Ca^{2+} cations occupy all sites I and the remaining 2 Na^+ cations locate at 2 out of the 3 sites II, leaving site III empty. Despite that 4 of the 6 8MR windows are obstructed by Na^+, *n*-hexane molecules are able to enter the α cages through the remaining open apertures and interact with the framework. However, its low pickup of *n*-hexane (0.44 mmol/g, ∼0.7 molecules per cage) indicates that most of the α cages are still inaccessible to *n*-hexane. Once the calcium exchange reaches 44.5%, 8 sites I accommodate 5 Na^+ and 3 Ca^{2+}. The remaining 1 Na^+ locates at site II, which frees 4 of the 6 8MR windows to be accessible to the *n*-hexane molecules. Our results suggest, upon increasing exchange to 44.5%, that nearly all α cages become accessible, leading to a sharp step in the amount of adsorption (see Table 4). As the degree of calcium exchange increases until there are no extraframework cations at site II (63.0% CaNa-A), the adsorbed amount of *n*-hexane reaches a plateau of 1.45 mmol/g (2.4 molecules per cage). Beyond this point, the amount of *n*-hexane adsorption is no longer a function of calcium content, indicating that the central cavities are entirely accessible.

Immersion of zeolite A is a complex process involving various interactions of guest *n*-hexane molecules with the external surface (wetting), with the framework (guest−host), and with other confined *n*-hexane molecules (guest−guest). These interactions produce exothermic heat effects labeled as, ΔH_{wet}, $\Delta H_{g\text{-}h}$, and $\Delta H_{g\text{-}g}$, respectively. Therefore, the overall interaction enthalpy, $\Delta H_{int\text{-}tot}$, can be represented by eq 1.

$$\Delta H_{int\text{-}tot} = \Delta H_{wet} + \Delta H_{g\text{-}h} + \Delta H_{g\text{-}g} \quad (1)$$

The magnitude of ΔH_{wet}, which is equal to $\Delta H_{int\text{-}tot}$ of Na-A (−2.90 kJ/mol - hexane), suggests a weak interaction. By

Table 3. TPD−MS Quantitative Analysis for Water and *n*-Hexane on Zeolite CaNa-A Samples

zeolite	$m_{equ\text{-}zeolite}$[a], mg	x[b], wt %	w_{tot}[c], mg	A_{H_2O}[d]	A_{-OH}[e]	A_{CO_2}[f]	w_{H_2O}[g], mg	w_{hex}[h], mg	x[i], g/g
34.8%CaNa-A	13.91	11.88	1.65	15.18	85.56	3.38	1.13	0.52	0.038
63.0%CaNa-A	20.22	14.99	3.03	11.55	62.95	4.42	0.81	2.22	0.125

[a]Weight of samples equilibrated under *n*-hexane vapor at 25 °C. [b]TGA weight loss (on the basis of the *n*-hexane equilibrated samples) related to the integral temperature region. [c]Total weight loss of samples related to the integral temperature region. [d]Relative integral area for the three H_2O peaks on the MS profiles. [e]Relative integral area for the three −OH group peaks on the MS profiles. [f]Relative integral area for CO_2 peaks on the MS profiles. [g]Amount of water released from zeolite samples. [h]Amount of *n*-hexane released from zeolite samples. [i]Amount of confined *n*-hexane relative to dehydrated zeolite A.

dx.doi.org/10.1021/jp508514e | J. Phys. Chem. C 2014, 118, 25590−25596

Table 4. Immersion and Interaction Enthalpies of Dehydrated Zeolites Na-A and CaNa-A with *n*-Hexane at 25 °C

zeolite	ΔH_{imm}[a] (J/g)	ΔH_{imm}[a] (kJ/mol - TO_2)	Q_c (mmol/g)[c]	$\Delta H_{int\text{-}tot}$[h] (kJ/mol - hexane)
Na-A	−5.59 ± 0.35(4)[b]	−0.39 ± 0.025	1.93[d], 0[e]	−2.90 ± 0.18[i]
34.8%CaNa-A	−11.92 ± 1.22(6)[b]	−0.82 ± 0.084	0.44, 0.43[e,f]	−27.76 ± 2.84
44.5%CaNa-A	−57.18 ± 1.29(8)[b]	−4.06 ± 0.091	1.36[e]	−42.12 ± 0.95
63.0%CaNa-A	−58.45 ± 3.33(8)[b]	−4.08 ± 0.23	1.45, 1.45[e,g]	−40.30 ± 2.30
76.2%CaNa-A	−58.70 ± 2.96(8)[b]	−4.12 ± 0.21	1.45[e]	−40.47 ± 2.04
97.9%CaNa-A	−58.94 ± 2.65(8)[b]	−4.12 ± 0.18	1.45[e]	−40.64 ± 1.83

[a]Enthalpies of immersion relative to dehydrated zeolite A. [b]Number of measurements. [c]The adsorption amount of *n*-hexane in zeolite A at 25 °C. [d]Wetting amount of *n*-hexane in zeolite A obtained from ref 32. [e]Adsorption amounts of *n*-hexane from ref 27. [f]Zeolite CaNa-A sample with a degree of Ca exchange of 34.3%. [g]Zeolite CaNa-A sample with a degree of Ca exchange of 64.0%. [h]Overall interaction enthalpies containing ΔH_{wet}, $\Delta H_{g\text{-}h}$, and $\Delta H_{g\text{-}g}$. [i]Enthalpies of interaction calculated using wetting amount of *n*-hexane in zeolite A.

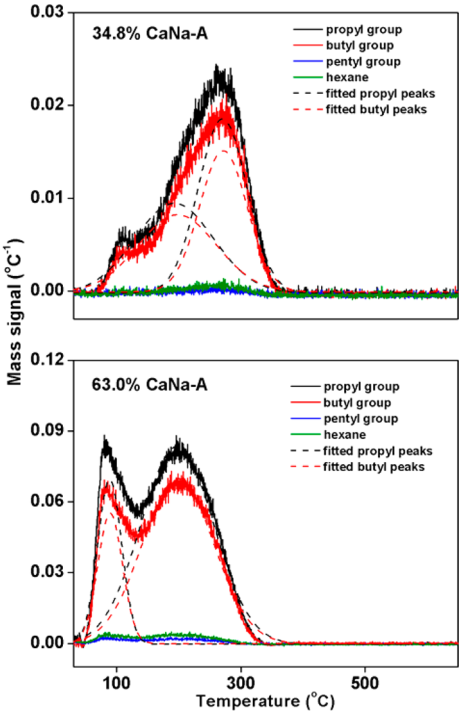

Figure 5. Mass spectroscopy (MS) profiles for *n*-hexane released from zeolites A (34.8% and 63.0% NaCa-A).

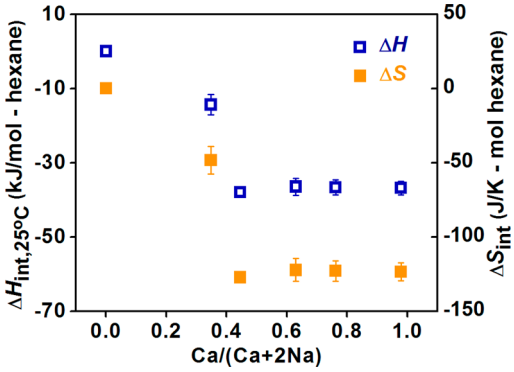

Figure 6. Enthalpy and entropy change for confinement of *n*-hexane in zeolite A as a function of calcium content.

subtracting wetting enthalpy ΔH_{wet} from the overall interaction enthalpy, eq 1 can be reduced to eq 2, which defines the overall enthalpy of interaction for confinement of *n*-hexane in the internal space of zeolite A, $\Delta H'_{int\text{-}tot}$ (Table 5).

$$\Delta H'_{int\text{-}tot} = \Delta H_{g\text{-}h} + \Delta H_{g\text{-}g} \quad (2)$$

For either Na-A or 34.8% CaNa-A, less than one hexane molecule is hosted per α cage (0 for Na-A and 0.7 for 34.8% CaNa-A), which implies that the $\Delta H_{g\text{-}g}$ is negligible since the guest−guest interaction is significant only at relatively high coverage (more than one molecule per cage), according to an exponential correlation of $\Delta H_{g\text{-}g} \propto n^x$ (n is number of guest molecules and x is between 2.5 and 3).[7] Hence, $\Delta H_{g\text{-}h}$ is around −14.4 kJ/mol - hexane, identical to the $\Delta H'_{int\text{-}tot}$ of 34.8% CaNa-A. On the other hand, as the degree of exchange increases from 0 (zeolite Na-A) to 34.8%, the α cage in zeolites evolves from inaccessible to partially accessible. Therefore, samples with more than 44.5% calcium exchange may accommodate 2.3−2.4 *n*-hexane molecules per cage, implying pronounced intermolecular interactions.[30] The calculated $\Delta H_{g\text{-}g}$ (−22.2 kJ/mol - hexane) is found to be roughly 70% of the heat of condensation for *n*-hexane (−31.56 kJ/mol - hexane at 25 °C[39]). Therefore, we successfully separate and quantify the contributions from various types of interactions, which are correlated to the properties (structure and type of cation) of the host framework as well as the population of confined guest molecules. These factors are energetically closely balanced and may be fine-tuned to achieve a particular functionality in industrial applications.

Since *n*-hexane confined in zeolite A is in equilibrium with pure *n*-hexane liquid under immersion at 25 °C, the change of chemical potential associated with inclusion of guest molecules is $\Delta\mu_{int} = \mu_{confined} - \mu_{liquid} = 0$. Therefore, according to $\Delta\mu = \Delta h - T\Delta s$, the entropy of confinement, relative to liquid hexane, can be calculated and is shown in Figure 6 as a function of calcium content. Hence, confinement of *n*-hexane is associated with a large exothermic enthalpy compensated by a strongly negative entropy. Indeed the enthalpy and entropy of confinement are linearly correlated; see Figure 7. Thus, stronger (more exothermic) enthalpy of interaction (confinement) may lead to more restricted molecular motion of *n*-hexane molecules in cages and may produce a more ordered arrangement of molecules than in the pure liquid and may result in a sharply diminished entropy. Spectroscopic studies (e.g., infrared and Raman spectroscopy and nuclear magnetic resonance) as well as inelastic neutron scattering may shed further light on the molecular nature of confinement and are suggested for future studies.

In summary, our study of confinement of *n*-hexane in calcium-exchanged zeolite A, a complex, yet well-defined, system, shows the impact of the degree of ion exchange (resulting in a change in pore size and accessibility) on guest−host interactions. We have determined not only the overall

dx.doi.org/10.1021/jp508514e | J. Phys. Chem. C 2014, 118, 25590−25596

Table 5. Interaction Enthalpies of *n*-Hexane with the External Surface (ΔH_{wet}), Framework ($\Delta H_{g\text{-}h}$), and Other Confined *n*-Hexane Molecules ($\Delta H_{g\text{-}g}$)

zeolite	$\Delta H'_{int\text{-}tot}$ [a] (kJ/mol - hexane)	ΔH_{wet} [b] (kJ/mol - hexane)	$\Delta H_{g\text{-}h}$ [c] (kJ/mol - hexane)	$\Delta H_{g\text{-}g}$ [d] (kJ/mol - hexane)
Na-A	0	−2.90 ± 0.18	N/A	N/A
34.8%CaNa-A	−14.39 ± 2.77	−2.90 ± 0.18	−14.39 ± 2.77	N/A
44.5%CaNa-A	−37.93 ± 0.95	−2.90 ± 0.18	−14.39 ± 2.77	−23.54 ± 1.29
63.0%CaNa-A	−36.46 ± 2.30	−2.90 ± 0.18	−14.39 ± 2.77	−22.07 ± 0.33
76.2%CaNa-A	−36.63 ± 2.04	−2.90 ± 0.18	−14.39 ± 2.77	−22.24 ± 0.52
97.9%CaNa-A	−36.79 ± 1.83	−2.90 ± 0.18	−14.39 ± 2.77	−22.40 ± 0.66

[a]Overall interaction enthalpies for confinement of *n*-hexane in the internal space of zeolite, after subtracting wetting enthalpy, ΔH_{wet}. [b]Wetting enthalpy calculated using wetting amount of *n*-hexane in zeolite A. The magnitude is defined by interaction enthalpy of Na-A. [c]Enthalpy of guest−host interaction with a magnitude defined by the increased exothermic enthalpy from Na-A to 34.8%CaNa-A. [d]Enthalpy of guest−guest interaction with a magnitude defined by the increased exothermic enthalpy from 34.8%CaNa-A to CaNa-A zeolites with ion exchange degree higher than 44.5%.

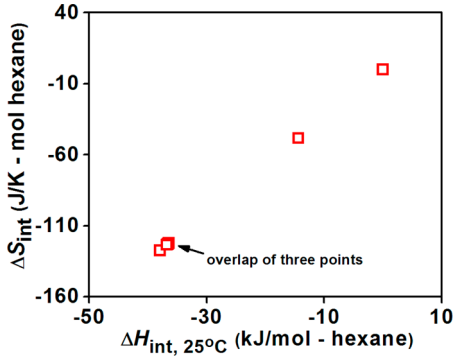

Figure 7. Enthalpy of interaction versus entropy change for confinement of *n*-hexane in Ca-exchanged zeolites A. Note that the four points with the most exothermic enthalpy and the lowest entropy in Figure 6 overlap in this figure.

trend and magnitude of energetics but also the contributions from various interactions (wetting, guest−host, and guest−guest). The interpretation confirms the crucial role of degree of calcium exchange on guest accessibility and suggests that all of these interactions should be considered in scientific research and industrial applications related to confinement/adsorption of organic molecules. Molecular modeling and direct experimental approaches (including calorimetric and spectroscopic) complement each other. We believe that a well-planned combination of both may greatly enhance the research quality and benefit the zeolite architects.

5. CONCLUSIONS

The guest−host interactions of a nonpolar organic hydrocarbon (*n*-hexane) with a series of Ca-exchanged zeolite A have been studied by immersion calorimetry coupled with temperature-programmed desorption and mass spectroscopy (TPD−MS). The interaction enthalpy is found to be a function of calcium content and can be separated into three types of contributions from wetting of the external surface (−2.9 kJ/mol - hexane), guest−host (−14.4 kJ/mol - hexane), and guest−guest intermolecular interactions (−22.2 kJ/mol - hexane).

AUTHOR INFORMATION

Corresponding Author

*E-mail: anavrotsky@ucdavis.edu (A.N.).

Author Contributions

[§]H. Sun and D. Wu contributed equally; all authors contributed to the interpretation of and writing the paper.

Notes

The authors declare no competing financial interest.

ACKNOWLEDGMENTS

H.S. is grateful to the National Natural Science Foundation of China for financial support under the National Natural Science Fund for Young Scholar (No. 21201063), the Ministry of Education of Republic of China for financial support under the Specialized Research Fund for the Doctoral Program of Higher Education of China (SRFDP) (No. 20110074120020) and the Fundamental Research Funds for the Central Universities, and the China Scholarship Council for the State Scholarship Fund (No. 201308310077). The calorimetric work was supported by the U.S. Department of Energy, Office of Basic Energy Sciences, grant DE-FG02-05ER15667.

REFERENCES

(1) Weitkamp, J.; Puppe, L. *Catalysis and Zeolites: Fundamentals and Applications*; Springer: Heidelberg, 1999.

(2) Auerbach, S. M., Carrado, K. A., Dutta, P. K., Eds. *Handbook of Zeolite Science and Technology*; Taylor & Francis: London, 2003.

(3) Corma, A. Inorganic Solid Acids and Their Use in Acid-Catalyzed Hydrocarbon Reactions. *Chem. Rev.* **1995**, *95*, 559−614.

(4) Chen, N. Y.; Gorwood, W. E.; Dwyer, F. G. *Shape Selective Catalysis in Industrial Applications*, 2nd ed.; Marcel Dekker, Inc.: New York, 1996.

(5) Ruthven, D. M. *Principles of Adsorption & Adsorption Processes*; John Wiley & Sons: New York, 1984.

(6) Bates, S. P.; vanWell, W. J. M.; vanSanten, R. A.; Smit, B. Energetics of *n*-alkanes in zeolites: A configurational-bias Monte Carlo investigation into pore size dependence. *J. Am. Chem. Soc.* **1996**, *118*, 6753−6759.

(7) Eder, F.; Lercher, J. A. Alkane sorption in molecular sieves: The contribution of ordering, intermolecular interactions, and sorption on Bronsted acid sites. *Zeolites* **1997**, *18*, 75−81.

(8) Bates, S. P.; van Well, W. J. M.; van Santen, R. A.; Smit, B. Location and conformation of *n*-alkanes in zeolites: An analysis of configurational-bias Monte Carlo calculations. *J. Phys. Chem-Us* **1996**, *100*, 17573−17581.

(9) Smit, B.; Maesen, T. L. M. Commensurate Freezing of Alkanes in the Channels of a Zeolite. *Nature* **1995**, *374*, 42−44.

(10) Zaborowski, E.; Zimmermann, H.; Vega, S. Molecular modeling and solid-state NMR of short-chain molecules in Dianin's compound and zeolite 5A. *J. Am. Chem. Soc.* **1998**, *120*, 8113−8123.

(11) Denayer, J. F.; Souverijns, W.; Jacobs, P. A.; Martens, J. A.; Baron, G. V. High-temperature low-pressure adsorption of branched C-5-C-8 alkanes on zeolite beta, ZSM-5, ZSM-22, zeolite Y, and mordenite. *J. Phys. Chem. B* **1998**, *102*, 4588−4597.

(12) Inel, O.; Topaloglu, D.; Askin, A.; Tumsek, F. Evaluation of the thermodynamic parameters for the adsorption of some hydrocarbon's

on 4A and 13X zeolites by inverse gas chromatography. *Chem. Eng. J.* **2002**, *88*, 255−262.
(13) Ramachandran, C. E.; Williams, B. A.; van Bokhoven, J. A.; Miller, J. T. Observation of a compensation relation for n-hexane adsorption in zeolites with different structures: implications for catalytic activity. *J. Catal.* **2005**, *233*, 100−108.
(14) Moreno-Pirajan, J. C.; Giraldo, L. Calorimetric study of mesoporous solids at room temperature. *Microporous Mesoporous Mater.* **2012**, *156*, 45−50.
(15) Wu, D.; Navrotsky, A. Small molecule − Silica interactions in porous silica structures. *Geochim. Cosmochim. Acta* **2013**, *109*, 38−50.
(16) Wu, D.; Hwang, S. J.; Zones, S. I.; Navrotsky, A. Guest-host interactions of a rigid organic molecule in porous silica frameworks. *Proc. Natl. Acad. Sci. U.S.A.* **2014**, *111*, 1720−1725.
(17) Pluth, J. J.; Smith, J. V. Accurate Redetermination of Crystal-Structure of Dehydrated Zeolite A. Absence of Near Zero Coordination of Sodium. Refinement of Silicon,Aluminum-Ordered Superstructure. *J. Am. Chem. Soc.* **1980**, *102*, 4704−4708.
(18) Porcher, F.; Souhassou, M.; Graafsma, H.; Puig-Molina, A.; Dusausoy, Y.; Lecomte, C. Refinement of framework disorder in dehydrated CaA zeolite from single-crystal synchrotron data. *Acta Crystallogr., Sect. B* **2000**, *56*, 766−772.
(19) Wu, D.; Gassensmith, J. J.; Gouvea, D.; Ushakov, S.; Stoddart, J. F.; Navrotsky, A. Direct Calorimetric Measurement of Enthalpy of Adsorption of Carbon Dioxide on CD-MOF-2, a Green Metal-Organic Framework. *J. Am. Chem. Soc.* **2013**, *135*, 6790−6793.
(20) Rosenbach, N.; Ghoufi, A.; Deroche, I.; Llewellyn, P. L.; Devic, T.; Bourrelly, S.; Serre, C.; Ferey, G.; Maurin, G. Adsorption of light hydrocarbons in the flexible MIL-53(Cr) and rigid MIL-47(V) metal-organic frameworks: A combination of molecular simulations and microcalorimetry/gravimetry measurements. *Phys. Chem. Chem. Phys.* **2010**, *12*, 6428−6437.
(21) Silva, J. A. C.; Da Silva, F. A.; Rodrigues, A. E. Separation of n/iso paraffins by PSA. *Sep. Purif. Technol.* **2000**, *20*, 97−110.
(22) Barcia, P. S.; Silva, J. A. C.; Rodrigues, A. E. Octane Upgrading of C-5/C-6 Light Naphtha by Layered Pressure Swing Adsorption. *Energ Fuels* **2010**, *24*, 5116−5130.
(23) Toulhoat, H.; Raybaud, P.; Benazzi, E. Effect of confinement on the selectivity of hydrocracking. *J. Catal.* **2004**, *221*, 500−509.
(24) Sastre, G.; Corma, A. The confinement effect in zeolites. *J. Mol. Catal. A: Chem.* **2009**, *305*, 3−7.
(25) Garcia, E. J.; Perez-Pellitero, J.; Jallut, C.; Pirngruber, G. D. Quantification of the confinement effect in microporous materials. *Phys. Chem. Chem. Phys.* **2013**, *15*, 5648−5657.
(26) Luhrs, H.; Derr, J.; Fischer, R. X. K and Ca exchange behavior of zeolite A. *Microporous Mesoporous Mater.* **2012**, *151*, 457−465.
(27) Sun, H. *Study on High-Performances Adsorbent Material for Improving Molecular Scale Management Functions of Naphtha*. Ph.D. Thesis, East China University of Science and Technology: Shanghai, 2009.
(28) Eder, F.; Stockenhuber, M.; Lercher, J. A. Bronsted acid site and pore controlled siting of alkane sorption in acidic molecular sieves. *J. Phys. Chem. B* **1997**, *101*, 5414−5419.
(29) Daems, I.; Baron, G. V.; Punnathanam, S.; Snurr, R. Q.; Denayer, J. F. M. Molecular cage nestling in the liquid-phase adsorption of n-alkanes in 5A zeolite. *J. Phys. Chem. C* **2007**, *111*, 2191−2197.
(30) Silva, J. A. C.; Rodrigues, A. E. Equilibrium and kinetics of n-hexane sorption in pellets of 5A zeolite. *AIChE J.* **1997**, *43*, 2524−2534.
(31) Silva, J. A. C.; Rodrigues, A. E. Multisite Langmuir model applied to the interpretation of sorption of n-paraffins in 5A zeolite. *Ind. Eng. Chem. Res.* **1999**, *38*, 2434−2438.
(32) Cao, J.; Shen, B. X. An Approach for Determining the Absolute Adsorption Capacity of n-Paraffin on 5A Molecular Sieve From Liquid Phase. *Pet. Sci. Technol.* **2011**, *29*, 1912−1921.
(33) Buszewski, B.; Krupczynska, K.; Gadzala-Kopciuch, R. M.; Rychlicki, G.; Kaliszan, R. Evaluation of HPLC columns: A study on surface homogeneity of chemically bonded stationary phases. *J. Sep. Sci.* **2003**, *26*, 313−321.
(34) Makowski, W.; Ogorzalek, L. Determination of the adsorption heat of n-hexane and n-heptane on zeolites beta, L, 5A, 13X, Y and ZSM-5 by means of quasi-equilibrated temperature-programmed desorption and adsorption (QE-TPDA). *Thermochim. Acta* **2007**, *465*, 30−39.
(35) Breck, D. W. *Zeolite Molecular Sieves*; Wiley: New York, 1974.
(36) Ogawa, K.; Nitta, M.; Aomura, K. A Theoretical Study of Site Selectivity of Zeolite Cation. 1. Site Selectivities of Alkali and Alkaline Earth Metal Cations in Zeolite A. *J. Phys. Chem* **1978**, *82*, 1655−1660.
(37) Pluth, J. J.; Smith, J. V. Crystal Structure of Dehydrated Ca-Exchanged Zeolite A. Absence of Near-Zero-Coordinate Ca^{2+} Ion. Presence of Al Complex. *J. Am. Chem. Soc.* **1983**, *105*, 1192−1195.
(38) Seff, K. Structural Chemistry inside Zeolite A. *Acc. Chem. Res.* **1976**, *9*, 121−128.
(39) Majer, V., Svoboda, V., Eds. *Enthalpies of Vaporization of Organic Compounds: A Critical Review and Data Compilation*; Blackwell Scientific Publications: Oxford, U.K., 1985.